



Two-proton emission systematicsD. S. Delion ^{1,2,3,4} and S. A. Ghinescu ^{1,2}¹“Horia Hulubei” National Institute of Physics and Nuclear Engineering, 30 Reactorului, POB MG-6, RO-077125, Bucharest-Măgurele, România²Department of Physics, University of Bucharest, 405 Atomîștilor, POB MG-11, RO-077125, Bucharest-Măgurele, România³Academy of Romanian Scientists, 3 Ilfov RO-050044, Bucharest, România⁴Bioterra University, 81 Gârlei RO-013724, Bucharest, România

(Received 9 January 2022; accepted 22 February 2022; published 7 March 2022)

The simultaneous emission of two protons is an exotic and complex three-body process. It is very important for experimental groups investigating the nuclear stability on the proton drip line to have a simple rule predicting the two-proton decay widths with a reasonable accuracy for transitions between ground as well as excited states in terms of relevant physical variables. In spite of its complexity, we show that the two-proton emission process obeys similar rules as for binary emission processes like proton, α , and heavy cluster decays. It turns out that the logarithm of the decay width, corrected by the centrifugal barrier, linearly depends upon the Coulomb parameter within one order of magnitude. On the other hand, the universal linear dependence with a negative slope between the logarithm of the reduced width and the fragmentation potential, valid for any kind of binary decay process, is also fulfilled for the two-proton emission with a relative good accuracy. As a consequence of pairing correlations the two protons are simultaneously emitted from a spin singlet paired state. We evidence that indeed one obtains a linear dependence between the logarithm of the reduced width and pairing gap within a factor of two, giving a good predictive power to this law. It turns out that the two-proton and alpha-cluster formation probabilities have similar patterns versus the pairing gap, while in the one-proton case one has a quasiconstant behavior.

DOI: [10.1103/PhysRevC.105.L031301](https://doi.org/10.1103/PhysRevC.105.L031301)

The proton drip line is mainly investigated by one- and two-proton emission processes [1–4]. The two-proton emission is a very exotic mode that is energetically possible in some nuclei. In the earlier 1960s Goldansky proposed two extreme mechanisms in which the particles are emitted, either simultaneously or sequentially [5]. The first systematic theoretical analysis of the processes involving the inherent three-body problem was performed in Ref. [6]. The theoretical description of two-proton emission was performed by using few-body formalism in terms of hyperspherical coordinates [7–9], as well as R -matrix approaches [10,11]. The Feshbach reaction theory and the continuum shell model were also applied [12,13]. The one-proton decay systematics reveals simple two-body features depending on the Coulomb and centrifugal parameters [14]. The systematic analysis indicates that the two-proton emission has a three-body character, between the diproton and pure sequential decay [15]. On the other hand, it is important to point out that the pairing interaction induces a clustering of the two protons. This is a fundamental property in α -emission, explaining the clustering of the four nucleons [16]. In the last years several investigations were performed in order to describe half-lives of the two-proton emission process by using effective liquid drop model [17], Gamow coupled channel approach [18], Gamow model with variable energy [19], semiempirical four-parameter [20] or two-parameter relation [21], and the

Gamow approach with square nuclear plus Coulomb potential [22].

In this paper we will show that the systematics of the two-proton emission has a similar universal feature compared to the usual binary decays, namely that the logarithm of the reduced width linearly decreases upon the increase of the fragmentation potential, defined as the difference between the top of the Coulomb barrier and Q value. On the other hand, as a consequence of the pairing correlations between emitted protons, the same quantity is directly proportional to the pairing gap.

Let us consider the two-proton emission process

$$P \rightarrow D + 2p. \quad (1)$$

Experimental data evidenced the quasisimultaneous detection of the emitted protons with equal energies. This allowed us to propose in Ref. [23] a simplified approach, where we have shown that the distribution of emitted protons is centered around the configuration with almost equal distances $r_1 \approx r_2$. This is a consequence of the initial condition given by the two-proton pairing wave function on the nuclear surface, centered around $r_1 = r_2$. Beyond the nuclear surface the diproton system becomes unstable. The interproton nuclear plus centrifugal plus Coulomb potential,

$$v(r) = -v_0 \exp\left(-\frac{r^2}{b^2}\right) + \frac{\hbar^2 l(l+1)}{2\mu_p r^2} + \frac{e^2}{r}, \quad (2)$$

TABLE I. Parameters of two-proton emission.

no.	Z_P	N_P	A_P	L	Q (MeV)	V_{frag} (MeV)	χ	ρ	$\log_{10} \gamma_{\text{exp}}^2$	$\log_{10} \Gamma_{\text{exp}}$ (MeV)	$\log_{10} \Gamma_1$ (MeV)	$\log_{10} \Gamma_2$ (MeV)	Ref.
1	4	2	6	0	1.370	0.316	1.248	1.014	-1.625	-1.041	-0.562	-1.230	[26]
2	6	2	8	0	2.110	1.010	2.133	1.443	-1.500	-0.881	-1.211	-1.322	[27]
3	7	3	10	1	1.300	2.381	3.508	1.239	-2.686	-3.701	-3.254	-3.207	[17]
4	8	4	12	0	1.640	2.577	3.825	1.488	-0.933	-1.241	-2.825	-2.536	[28]
5	12	7	19	0	0.750	5.514	9.769	1.170	-3.749	-10.121	-9.439	-9.137	[29]
6	17	11	28	2	1.970	6.556	9.211	2.128	-3.409	-8.391	-8.395	-7.937	[17]
7	19	13	32	2	2.080	7.262	10.208	2.273	-3.508	-9.091	-9.097	-8.667	[17]
8	26	19	45	0	1.154	10.938	19.533	1.864	-3.942	-18.941	-18.738	-18.755	[30]
9	28	20	48	0	1.350	11.535	19.593	2.053	-4.699	-19.261	-18.338	-18.426	[31]
10	29	23	52	4	0.770	12.337	26.986	1.585	-3.918	-30.701	-30.604	-30.794	[17]
11	30	24	54	0	1.480	11.980	20.201	2.221	-4.125	-18.911	-18.627	-18.732	[32]
12	31	26	57	2	2.050	11.697	17.795	2.654	-4.047	-16.041	-15.864	-15.889	[17]
13	36	31	67	0	1.690	13.763	23.041	2.520	-2.581	-19.641	-21.011	-21.332	[33]

is given in terms of the relative distance $r = r_1 - r_2$, angular momentum l , and reduced proton mass $\mu_p = m_p/2$. A simple estimate shows that one obtains a resonant state at a very small energy $E_{\text{res}} \approx 0.1$ MeV with a decay width $\log_{10} \Gamma_{\text{res}} \approx -2$ (MeV) for $l = 0$, $v_0 \approx 38$ MeV, $b \approx 1.8$ fm. Therefore the diproton “cluster” is weakly bound but its center of mass (c.m.) radius $R = \frac{1}{2}(r_1 + r_2)$ moves in the Coulomb field of the daughter nucleus as a real diproton particle. Thus, we suppose for the decay width a similar to the binary case expression, proportional to the scattering amplitude squared N_L^2 in some channel characterized by the angular momentum L [24]. It can be rewritten

$$\Gamma_L = \hbar v N_L^2 = \hbar v \frac{\gamma_L^2(R)}{G_L^2(\chi, \rho)} \equiv \gamma_L^2(R) P_L(\chi, \rho), \quad (3)$$

in terms of the reduced width $\gamma_L^2(R)$ and Coulomb penetrability $P_L(\chi, \rho)$. Let us mention that these quantities differ by a constant factor with respect to the standard definitions in Ref. [25]. The penetrability is defined by the irregular Coulomb wave function which has the following semiclassical representation:

$$G_L(\chi, \rho) = G_0(\chi, \rho) C_L(\chi, \rho). \quad (4)$$

Let us mention that the monopole and centrifugal terms are respectively given as

$$G_0(\chi, \rho) = (\cot \alpha)^{1/2} \exp[\chi(\alpha - \sin \alpha \cos \alpha)],$$

$$C_L(\chi, \rho) = \exp\left[\frac{L(L+1)}{\chi} \tan \alpha\right], \quad (5)$$

in terms of the dimensionless parameter

$$\cos^2 \alpha \equiv \frac{\rho}{\chi} = \frac{Q}{V_C(R)} = \frac{QR}{4Z_D e^2}, \quad (6)$$

depending upon the Coulomb parameter and reduced radius

$$\chi = \frac{4Z_D e^2}{\hbar v}, \quad \rho = \kappa R, \quad (7)$$

where

$$v = \sqrt{\frac{2Q}{\mu}}, \quad \hbar \kappa = \mu v. \quad (8)$$

The reduced width γ_L^2 is also called diproton formation probability. We will estimate it on the nuclear surface at the “geometrical touching configuration”

$$R = 1.2(A_D^{1/3} + A_{2p}^{1/3}). \quad (9)$$

Let us stress that this quantity includes the influence of the above defined dissociation probability of the diproton system Γ_{res} . In order to prove the validity of this “binary representation” we investigated the available experimental data, given in Table I.

Here, we give the charge Z_P , neutron N_P , and mass number A_P of the parent nucleus, angular momentum of the emitted diproton L , Q value, fragmentation potential

$$V_{\text{frag}} = V_C(R) - Q, \quad (10)$$

Coulomb parameter χ , reduced radius $\rho = \kappa R$ Eq. (7), experimental reduced width

$$\gamma_{\text{exp}}^2 = \frac{\Gamma_0}{P_L}, \quad (11)$$

where the monopole width Γ_0 is defined below by Eq. (12), and the logarithm of the experimental decay width $\Gamma_{\text{exp}} = \hbar \ln 2/T_{\text{exp}}$. We also included in the last two columns the two versions for computed decay widths, as described below by Eq. (18).

The most important ingredient defining the experimental reduced width (11) is the irregular Coulomb function depending on Coulomb parameter χ and reduced radius ρ . We have shown in recent Refs. [34–36] that the two regions of the one-proton emission systematics, divided by $Z = 68$, correspond to two different regions in the dependence between ρ and χ parameters. At the same time, one obtains a similar conclusion concerning the two regions of the α decay divided by the doubly magic nucleus ^{208}Pb . In Fig. 1(a) we extend this analysis by noticing a strong correlation between the two

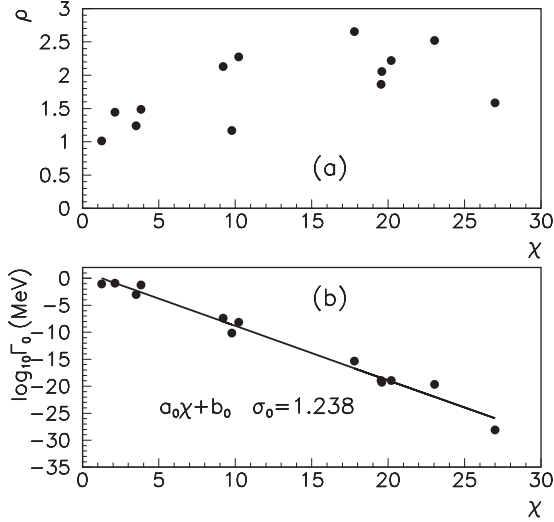


FIG. 1. (a) Reduced radius versus Coulomb parameter. (b) Logarithm of the monopole decay width versus the Coulomb parameter. The fit parameters are given in the first line of Table II.

quantities, except the two lower points, corresponding to the cases 4 and 13 in Table I, which indeed will appear separately in our systematics.

Then we analyzed to what extent the Geiger-Nuttall law, expressing the linear relation between the logarithm of the decay with and Coulomb parameter, is fulfilled. To this purpose we extracted the influence of the centrifugal barrier by defining the monopole decay width [14]

$$\Gamma_0 = \Gamma_{\text{exp}} C_L^2(\chi, \rho). \quad (12)$$

In Fig. 1(b) we notice such a linear dependence

$$\log_{10} \Gamma_0 \approx a_0 \chi + b_0, \quad (13)$$

on a wide interval of almost 30 orders of magnitude.

In the first line of Table II we give the parameters of the fit line with an overall root mean square (rms) error $\sigma_0 = 1.238$. Notice a slightly smaller rms error $\sigma'_0 = 1.010$ by excluding the two above-mentioned cases 4 and 13.

Let us stress that this is a rather large error, corresponding to more than one order of magnitude. Therefore this law has an approximate character and a poor predictive power. This is due to the variation of the reduced width γ_L^2 along the analyzed emitters.

In order to further analyze this feature let us mention that in all binary emission processes we evidenced in Refs. [15,34,35] an analytical universal law for reduced

TABLE II. Parameters of the fit lines.

k	a_k	b_k	σ_k	σ'_k
0	-1.009	1.272	1.238	1.010
1	-0.183	-1.757	0.742	0.396
2	0.622	-4.876	0.702	0.333

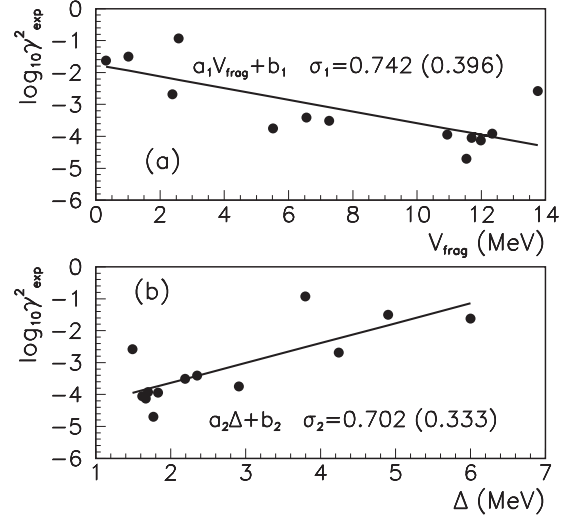


FIG. 2. Logarithm of the experimental reduced width at the geometrical touching radius $R = 1.2(A_D^{1/3} + 2^{1/3})$ versus the fragmentation potential (a) and pairing gap (b). The fit parameters are given in the second line of Table II. The rms error in parentheses corresponds to the analysis without considering cases 4 and 13.

widths

$$\log_{10} \gamma^2 = -\frac{\pi \log_{10} e}{\hbar \omega_1} V_{\text{frag}} + \log_{10} s, \quad (14)$$

in terms of the harmonic oscillator frequency of the internal nuclear interaction approximated by an inverted parabola $\hbar \omega_1$ and the spectroscopic factor s . We plot in Fig. 2(a) the logarithm of the experimental reduced width versus the fragmentation potential. This dependence can satisfactorily be fitted by a straight line

$$\log_{10} \gamma_{\text{exp}}^2 \approx a_1 V_{\text{frag}} + b_1 \quad (15)$$

with a negative slope $a_1 < 0$. The overall rms error in the second line of Table II corresponds to a factor of 5 and to a factor of 2.5 if one excludes the cases 4 and 13, corresponding to the upper two points. The fit parameters lead to the following values in Eq. (14) $\hbar \omega_1 = 7.456$ MeV, $s = 0.017$. Notice that we obtained the same order of magnitude, namely $\hbar \omega_1 = 11.389$ MeV ($A < 145$), 12.580 MeV ($A > 145$) in the case of the Woods-Saxon potential used to describe one-proton emission and $\hbar \omega_1 = 9.080$ MeV for double-folding potential describing α decay [36].

Let us mention here that in Ref. [23] we estimated the experimental two-proton formation probability on the nuclear surface within the pairing BCS approach for ^{45}Fe (corresponding to no. 8 in Table I) as being $\log_{10} \gamma_{\text{BCS}}^2 \approx -2$. From Fig. 2(a) we notice that for $V_{\text{frag}} = 10.938$ MeV one obtains $\log_{10} \gamma_{\text{exp}}^2 \approx -4$. The missing two orders of magnitude we can ascribe to the above mentioned penetration of the diproton system through the interproton potential (2).

In the same reference we evidenced that the two-proton formation probability quadratically depends upon the pairing gap

$$\gamma_{\text{BCS}}^2 \approx (uv)^2 \approx \Delta^2, \quad (16)$$

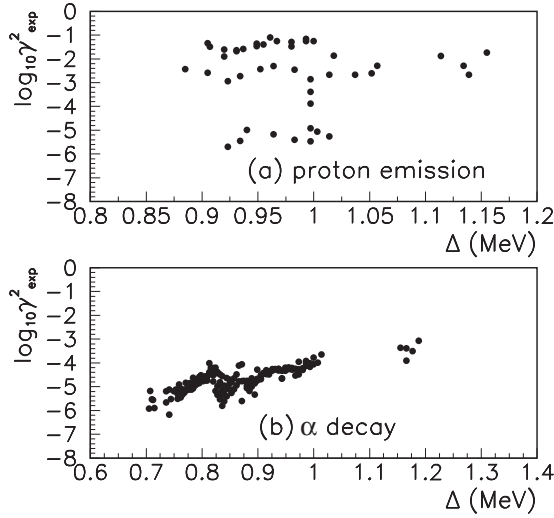


FIG. 3. Logarithm of the experimental reduced width versus the pairing gap for one-proton emission (a) and α decay from even-even emitters (b).

where u and v denote the standard BCS amplitudes. Anyway, the systematic analysis of two-proton emitters in Table I evidenced that the exponential dependence upon the pairing gap provides a significantly smaller rms error. Thus, we plotted in Fig. 2(b) the dependence between the logarithm of the experimental reduced width and the systematic rule of the pairing gap $\Delta = 12A^{-1/2}$,

$$\log_{10} \gamma_{\text{exp}} \approx a_2 \Delta + b_2. \quad (17)$$

Notice the linear correlation with a rms error in the third line of Table II corresponding to a factor of three. One obtains a better agreement within a factor of two if one excludes the two mentioned cases 4 (magic in neutrons) and 13.

Let us mention in this context that the situation is quite different in the case of one-proton emission. In Fig. 3(a) we plotted the experimental reduced width defined by Eq. (11) [35] versus the pairing gap. One sees that the upper and lower regions practically do not depend upon the pairing gap. Notice that the “vertical” transitional region around $\Delta \approx 1$ MeV corresponds to Tm isotopes [35].

This is due to the fact that the one-proton formation probability has a one-particle character, being proportional to the BCS amplitude squared u_F^2 at the Fermi level. In the case of the α decay from even-even emitters the behavior is similar to the two-proton emission, as seen in panel (b) of the same figure, where we notice two parallel linear dependencies divided by the doubly magic nucleus ^{208}Pb . Therefore the formation probability of the two-proton and alpha cluster has a common collective pairing nature, in spite of the fact that the first system is weakly bound, while the second one is strongly bound.

The influence of the quadrupole deformation can be estimated by using the Fröman method as in Ref. [37]. Thus, the influence of the non-diagonal matrix elements of the Fröman matrix is rather small, being about 15% for two-proton emitters at $\beta = 0.3$.

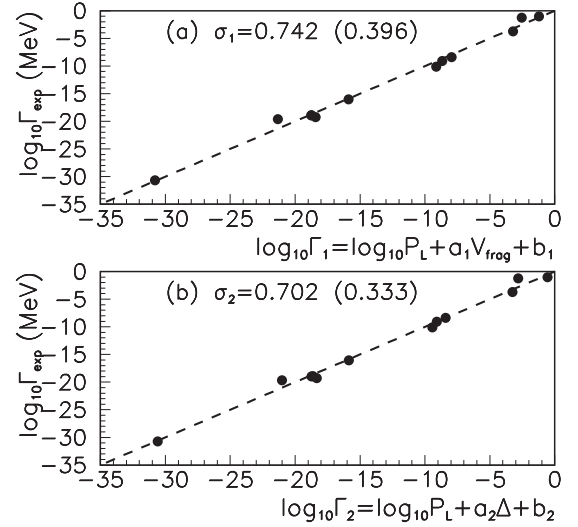


FIG. 4. Logarithm of the experimental decay width versus $\log_{10} \Gamma_1 = \log_{10} P_L + a_1 V_{\text{frag}} + b_1$ (a) and $\log_{10} \Gamma_2 = \log_{10} P_L + a_2 \Delta + b_2$ (b). The fit parameters are given in the third line of Table II. The rms error in parentheses corresponds to the analysis without considering cases 4 and 13.

Finally we analyzed the experimental decay width by plotting in Fig. 4 its logarithm as a function of the theoretical width for panels (a) and (b), respectively:

$$\log_{10} \Gamma_1 = \log_{10} P_L + a_1 V_{\text{frag}} + b_1, \quad (18a)$$

$$\log_{10} \Gamma_2 = \log_{10} P_L + a_2 \Delta + b_2, \quad (18b)$$

The values of the theoretical predictions are given in the last two columns of Table I and the fit parameters in the last two lines of Table II. Notice the very good linear correlation between these quantities along the first bisectrices plotted by a dashed line.

Concluding, in spite of the fact that the two-proton emission is a three-body process, we evidenced the binary character of laws connecting the logarithm of the decay widths in terms some physical quantities. Thus, we evidenced the linear correlation between the logarithm of the reduced width and the fragmentation potential with a negative slope, predicted as an analytical universal rule for binary emission processes like one-proton emission, α , and heavy cluster decays. On the other hand, we also evidenced the role played by the pairing interaction, given by the linear correlation between the logarithm of the reduced width and pairing gap, as predicted by microscopic estimates of the two-proton formation probability. The relative small rms error give a powerful predictive power to this last rule. The two-proton and α -cluster formation probabilities have similar patterns versus the pairing gap, while in the one-proton emission one has a quasiconstant behavior.

ACKNOWLEDGMENTS

This work was supported by the grant of the Romanian Ministry Education and Research No. PN-18090101/2019-2021 and by Grant No. 01-3-1136-2019/2023 of JINR-Dubna.

- [1] P. J. Woods and C. N. Davids, *Annu. Rev. Nucl. Part. Sci.* **47**, 541 (1997).
- [2] A. A. Sonzogni, *Nucl. Data Sheets* **95**, 1 (2002).
- [3] D. S. Delion, R. J. Liotta, and R. Wyss, *Phys. Rep.* **424**, 113 (2006).
- [4] M. Pfützner, M. Karny, L. V. Grigorenko, and K. Riisager, *Rev. Mod. Phys.* **84**, 567 (2012).
- [5] V. I. Goldansky, *Nucl. Phys.* **19**, 482 (1960).
- [6] P. Swan, *Rev. Mod. Phys.* **37**, 336 (1965).
- [7] L. V. Grigorenko, R. C. Johnson, I. G. Mukha, I. J. Thompson, and M. V. Zhukov, *Phys. Rev. C* **64**, 054002 (2001).
- [8] L. V. Grigorenko and M. V. Zhukov, *Phys. Rev. C* **68**, 054005 (2003), and references therein.
- [9] L. V. Grigorenko, I. A. Egorova, M. V. Zhukov, R. J. Charity, and K. Miernik, *Phys. Rev. C* **82**, 014615 (2010).
- [10] R. A. Kryger, A. Azhari, M. Hellström, J. H. Kelley, T. Kubo, R. Pfaff, E. Ramakrishnan, B. M. Sherrill, M. Thoennessen, S. Yokoyama, R. J. Charity, J. Dempsey, A. Kirov, N. Robertson, D. G. Sarantites, L. G. Sobotka, and J. A. Winger, *Phys. Rev. Lett.* **74**, 860 (1995).
- [11] B. A. Brown and F. C. Barker, *Phys. Rev. C* **67**, 041304(R) (2003), and references therein.
- [12] J. Rotureau, J. Okolowicz, and M. Ploszajczak, *Phys. Rev. Lett.* **95**, 042503 (2005).
- [13] J. Rotureau, J. Okolowicz, and M. Ploszajczak, *Nucl. Phys. A* **767**, 13 (2006).
- [14] D. S. Delion, R. J. Liotta, and R. Wyss, *Phys. Rev. Lett.* **96**, 072501 (2006).
- [15] D. S. Delion, *Phys. Rev. C* **80**, 024310 (2009).
- [16] F. A. Janouch and R. J. Liotta, *Phys. Rev. C* **27**, 896 (1983).
- [17] M. Goncalves, N. Teruya, O. Tavares, and S. Duarte, *Phys. Lett. B* **774**, 14 (2017).
- [18] S. M. Wang and W. Nazarewicz, *Phys. Rev. Lett.* **120**, 212502 (2018).
- [19] O. A. P. Tavares and E. L. Medeiros, *Eur. Phys. J. A* **54**, 65 (2018).
- [20] I. Sreeja and M. Balasubramaniam, *Eur. Phys. J. A* **55**, 33 (2019).
- [21] H.-M. Liu, Y.-T. Zou, X. Pan, J.-L. Chen, B. He and X.-H. Li, *Chin. Phys. C* **45**, 024108 (2021).
- [22] Y.-B. Liu and S. Moretti *Chin. Phys. C* **45**, 043110 (2021).
- [23] D. S. Delion, R. J. Liotta, and R. Wyss, *Phys. Rev. C* **87**, 034328 (2013).
- [24] D. S. Delion, *Theory of Particle and Cluster Emission* (Springer-Verlag, Berlin/New York, 2010).
- [25] A. M. Lane and R. G. Thomas, *Rev. Mod. Phys.* **30**, 257 (1958).
- [26] W. Whaling, *Phys. Rev.* **150**, 836 (1966).
- [27] R. J. Charity, J. M. Elson, J. Manfredi, R. Shane, L. G. Sobotka, B. A. Brown, Z. Chajecski, D. Coupland, H. Iwasaki, M. Kilburn, Jenny Lee, W. G. Lynch, A. Sanetullaev, M. B. Tsang, J. Winkelbauer, M. Youngs, S. T. Marley, D. V. Shetty, A. H. Wuosmaa, T. K. Ghosh, and M. E. Howard, *Phys. Rev. C* **84**, 014320 (2011).
- [28] M. F. Jager, R. J. Charity, J. M. Elson, J. Manfredi, M. H. Mahzoon, L. G. Sobotka, M. McCleskey, R. G. Pizzone, B. T. Roeder, A. Spiridon, E. Simmons, L. Trache, and M. Kurokawa, *Phys. Rev. C* **86**, 011304(R) (2012).
- [29] I. Mukha (for the S271 Collaboration), *Eur. Phys. J. A* **42**, 421 (2009).
- [30] K. Miernik, W. Dominik, Z. Janas, M. Pfützner, L. Grigorenko, C. R. Bingham, H. Czyrkowski, M. Ćwiok, I. G. Darby, R. Dąbrowski, T. Ginter, R. Grzywacz, M. Karny, A. Korgul, W. Kuśmierz, S. N. Liddick, M. Rajabali, K. Rykaczewski, and A. Stolz, *Phys. Rev. Lett.* **99**, 192501 (2007).
- [31] C. Dossat, A. Bey, B. Blank, G. Canchel, A. Fleury, J. Giovinazzo, I. Matea, F. de Oliveira Santos, G. Georgiev, S. Grévy, I. Stefan, J.C. Thomas, N. Adimi, C. Borcea, D. Cortina Gil, M. Caamano, M. Stanoiu, F. Aksouh, B. A. Brown, and L. V. Grigorenko, *Phys. Rev. C* **72**, 054315 (2005).
- [32] B. Blank, A. Bey, G. Canchel, C. Dossat, A. Fleury, J. Giovinazzo, I. Matea, N. Adimi, F. De Oliveira, I. Stefan, G. Georgiev, S. Grévy, J. C. Thomas, C. Borcea, D. Cortina, M. Caamano, M. Stanoiu, F. Aksouh, B. A. Brown, F. C. Barker, and W. A. Richter, *Phys. Rev. Lett.* **94**, 232501 (2005).
- [33] T. Goigoux *et al.*, *Phys. Rev. Lett.* **117**, 162501 (2016).
- [34] D. S. Delion and A. Dumitrescu, *Phys. Rev. C* **102**, 014327 (2020).
- [35] D. S. Delion and A. Dumitrescu, *Phys. Rev. C* **103**, 054325 (2021).
- [36] A. Dumitrescu and D. S. Delion, *At. Data Nucl. Data Tables* (2022) (unpublished).
- [37] S. A. Ghinescu and D. S. Delion, *J. Phys. G: Nucl. Part. Phys.* **48**, 105108 (2021).